

Article

Non-Solvent- and Temperature-Induced Phase Separations of Polyaurolactam Solutions in Benzyl Alcohol as Methods for Producing Microfiltration Membranes

Svetlana O. Ilyina^{1,2}, Tatyana S. Anokhina¹ and Sergey O. Ilyin^{1,*} 

¹ A.V. Topchiev Institute of Petrochemical Synthesis, Russian Academy of Sciences, 29 Leninsky Prospect, 119991 Moscow, Russia

² Department of Plastics Processing Technology, D. Mendeleev University of Chemical Technology of Russia, 9 Miusskaya Square, 125047 Moscow, Russia

* Correspondence: s.o.ilyin@gmail.com; Tel.: +7-(916)-8276852

Abstract: The possibility of obtaining porous films through solutions of polyaurolactam (PA12) in benzyl alcohol (BA) was considered. The theoretical calculation of the phase diagram showed the presence of the upper critical solution temperature (UCST) for the PA12/BA system at 157 °C. The PA12 completely dissolved in BA at higher temperatures, but the resulting solutions underwent phase separation upon cooling down to 120–140 °C because of the PA12's crystallization. The viscosity of the 10–40% PA12 solutions increased according to a power law but remained low and did not exceed 5 Pa·s at 160 °C. Regardless of the concentration, PA12 formed a dispersed phase when its solutions were cooled, which did not allow for the obtention of strong films. On the contrary, the phase separation of the 20–30% PA12 solutions under the action of a non-solvent (isopropanol) leads to the formation of flexible microporous films. The measurement of the porosity, wettability, strength, permeability, and rejection of submicron particles showed the best results for a porous film produced from a 30% solution by non-solvent-induced phase separation. This process makes it possible to obtain a membrane material with a 240 nm particle rejection of 99.6% and a permeate flow of 1.5 kg/m²hbar for contaminated water and 69.9 kg/m²hbar for pure water.

Keywords: polyamide; polymer solution; viscosity; phase separation; microfiltration membrane



Citation: Ilyina, S.O.; Anokhina, T.S.; Ilyin, S.O. Non-Solvent- and Temperature-Induced Phase Separations of Polyaurolactam Solutions in Benzyl Alcohol as Methods for Producing Microfiltration Membranes. *Colloids Interfaces* **2023**, *7*, 10. <https://doi.org/10.3390/colloids7010010>

Academic Editors: Olga Milyaeva and Alexey Bykov

Received: 19 December 2022

Revised: 15 January 2023

Accepted: 18 January 2023

Published: 20 January 2023



Copyright: © 2023 by the authors. Licensee MDPI, Basel, Switzerland. This article is an open access article distributed under the terms and conditions of the Creative Commons Attribution (CC BY) license (<https://creativecommons.org/licenses/by/4.0/>).

1. Introduction

The use of membranes has become an integral part of many technological operations in different industrial areas. The most important segments of the membrane materials market are the petrochemical industry [1,2], water treatment [3,4], and gas separation [5,6]. In addition, membranes have found applications in medicine as various dressing materials [7], fetal membranes [8], membranes for hemodialysis in artificial kidneys [9,10], and membranes for the separation of biological solutions [11,12].

A membrane is the thinnest film that can selectively allow small particles to pass through itself while trapping and filtering out larger ones. The selectivity depends on the chemical nature of the membrane material and pore size, allowing for separating even the smallest objects, down to molecules, ions, or nanoscale particles. In this regard, there is a distinction between microfiltration (pore diameter: 50–500 nm), ultrafiltration (2–50 nm), and nanofiltration (≤ 2 nm) membranes [13,14]. Membranes with small and medium pore sizes are effective for separating and purifying low molecular weight liquids, such as hydrocarbons and water. Membranes with larger pores are used to purify liquids from solids and also as a support material for a small-porous selective layer [15].

In addition to porous membranes, there are nonporous materials with a filtration mechanism based on the principle of molecular diffusion [16]. These membranes are characterized by the presence of a dense selective layer, which allows for increased strength characteristics and, thus, an extended service life compared to conventional porous membranes.

Nonporous membranes are impermeable to particles and ions but are capable of allowing individual small molecules to pass under high pressures applied to a filtered medium. They are used in gas separation, pervaporation, and reverse osmosis processes [17–19].

Different organic and inorganic materials can be used for the production of membranes, provided that they can be turned into a thin film. Both types of membrane materials have their advantages and disadvantages when compared [20,21]. Inorganic materials include ceramics, zeolites, metals, and allotropic modifications of carbon such as graphene. Membranes based on them are considered to be more selective and permeable, resistant to adverse conditions, mechanically strong, and wear resistant [15]. However, a significant disadvantage of inorganic membranes is brittleness under impact loads and bending and the high cost of synthesis, which is also an obstacle to their widespread distribution [22,23].

Organic membranes are made mainly from polymers. A variety of polymer materials and the possibility of combining them mutually allow widely varying barrier properties and structures of membranes by introducing functional groups into the polymer composition. Organic membranes were originally developed based on cellulose and its derivatives [24]. Cellulose has become the most popular because of its wide availability and strong intra- and intermolecular hydrogen bonds, which make it resistant to many solvents [25,26]. Due to the positive properties of cellulose, many variants of cellulose-based membranes have been developed for various purposes [27–31]. In addition to natural cellulose, membranes are made from synthetic polymers, such as polyacrylonitrile [32,33], polyethersulfone [34], polysulfone [35], polyethylene, and polypropylene, and many other polymers [36,37].

Among a large number of methods of obtaining porous membranes, the method of the phase separation of polymer solutions has the greatest industrial applicability [38]. In this case, a two-phase system is formed in which the phase with a higher polymer content forms a porous film, and the phase with a lower polymer content generates pores [39,40]. The process of porous structure formation can be triggered in the following several methods [41–44]:

1. By immersion of a polymer solution in a bath with a non-solvent (a precipitant), where the membrane is formed due to the mass exchange of solvent and non-solvent [45–47]. The enrichment of the polymer solution with the non-solvent causes precipitation of the polymer, forming a membrane with a typically asymmetric structure that includes a dense surface layer (a skin) and a highly porous inner layer [48].
2. By evaporating a solvent from a three-component solution that also contains a polymer and a small percentage of a non-solvent that is less volatile than the solvent. When heated, the solvent evaporates faster, and the system undergoes phase separation with the formation of a porous structure due to the gradual increase in the concentration of non-solvent [49].
3. By precipitation using the non-solvent-rich vapor phase, which can additionally be saturated with a solvent if it is highly volatile. Polymer precipitation and membrane formation occur due to the diffusion of the vaporous non-solvent into the polymer solution [50,51].
4. By thermally induced phase separation due to the cooling of the solution prepared at a temperature higher than UCST [52–54]. In this case, cooling of the solution can be carried out in a cold bath with the same solvent, which can be used repeatedly.

Figure 1 summarizes the methods for producing polymer membranes via polymer solutions and the typical polymers previously used [13,45,51,55–58].

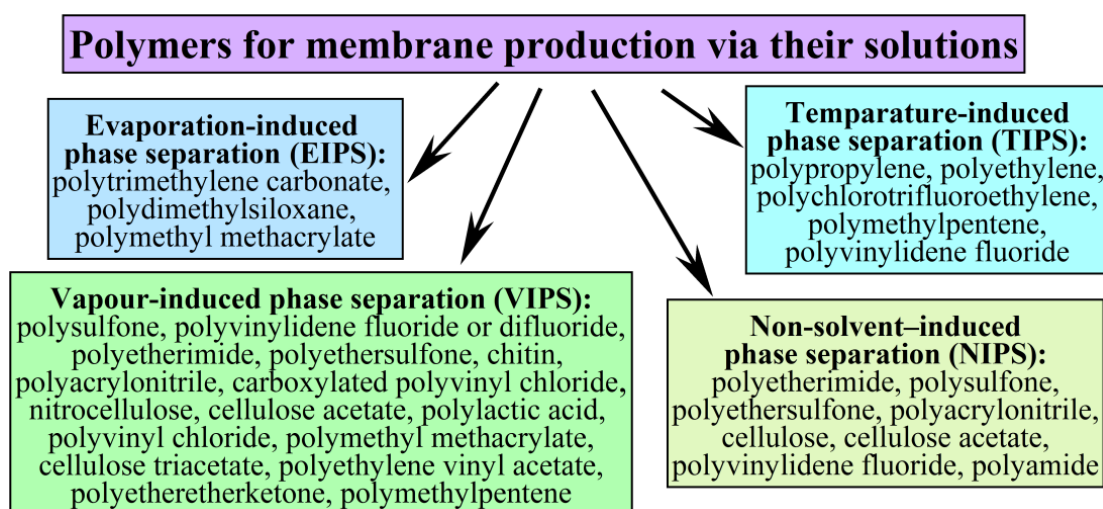


Figure 1. Methods for obtaining membranes from polymer solutions and the polymers used.

Polymer membranes must not only meet the requirements for their degree of permeability and selectivity but also be chemically resistant and inert to the filtered substance and surrounding equipment. The high reactivity of the membrane material leads to various defects on its surface and the destruction of the porous layer over time, which negatively affects the separation ability and service life. It is therefore relevant to use inert polymers, such as aromatic polyamide [59], polyketone [60], polytetrafluoroethylene [61,62], and polymethylpentene [63,64], to work in chemically aggressive environments and at high temperatures. Aliphatic polyamides (nylons) are similarly characterized by a high chemical resistance but may have strong hydrophilic properties [65,66]. This applies to polyamides, such as polycaprolactam (PA6) and poly(hexamethylene adipamide) (PA66), membranes from which are less suitable for cleaning water and aqueous solutions due to the fact of swelling and subsequent loss of mechanical strength. In addition, these polyamides are not resistant to alcohols, acids, and strong oxidizing agents [67]. It is therefore advisable to use more hydrophobic polyamides, such as polyundecanolactam (PA11) or polylauro lactam (PA12), to produce chemical- and water-resistant membranes. Both of these polymers can be obtained from natural renewable raw materials (e.g., vegetable oils [68,69]), but PA12 is more hydrophobic, which determines its better suitability as a highly resistant membrane material.

The thermal and chemical resistance of PA12 is due to the fact of strong intermolecular interactions caused by hydrogen bonds between the amide groups. As a consequence, strong solvents, such as hexafluoroisopropanol [70] or *m*-cresol [71,72], which are highly toxic and dangerous to the environment and humans, must be used to dissolve PA12. Therefore, there is a problem with selecting an effective and safe solvent when obtaining polyamide membranes from solution.

Such a solvent can be benzyl alcohol (BA), in which PA12 dissolves at high temperatures. BA has low volatility, nontoxicity [73], and easy biodegradability [74]. BA is used widely as a food additive [75], local anesthetic [76], antiseptic [77], a component of lotions for the treatment of pediculosis [78], and preservative for cosmetic products [79]. In this respect, BA can be regarded as a green solvent safe for industrial applications.

The possibility of obtaining nonporous and porous ultrafiltration membranes from PA12 has been previously shown by the thermally induced phase separation of its solutions, mainly in *m*-cresol or formic acid [80–83]. However, there have been no attempts to obtain polyamide membranes using BA as a solvent so far. In addition, there are no data on the solubility of PA12 in BA, the rheological behavior of its solutions, and the features of their phase separation upon cooling or the addition of a non-solvent. At the same time, this knowledge could be useful for developing safer methods of producing chemically resistant polyamide membranes using environmentally friendly materials. On this basis,

the purpose of this study was to evaluate the possibility of obtaining membrane materials from solutions of polylactolactam in benzyl alcohol and to study the morphological features of the resulting materials.

2. Materials and Methods

2.1. Materials

Poly(lactolactam) PA 12-E, produced by Anid (Yekaterinburg, Russia), with a melting point of 178 °C was used as a membrane material. Its intrinsic viscosity in *m*-cresol at 25 °C was 1.221 dL/g, corresponding to a weight average molecular mass of 3.47×10^4 g/mol [72]. Benzyl alcohol ($\geq 99.0\%$) was supplied by Fluka (Buchs, Switzerland), while isopropyl alcohol (99.8%) was produced by EKOS-1 (Moscow, Russia).

2.2. Obtaining Porous Films

The PA12/BA solutions were prepared at 180 °C with stirring on a magnetic stirrer IKA C-MAG HS 7 (Staufen, Germany). The PA12 concentrations were 10, 15, 20, 25, 30, 35, and 40 wt.%.

The films were prepared on an HLCL-1000 laminator (ChemInstruments, West Chester Township, OH, USA) by applying a hot polymer solution between the layers of polyimide siliconized film at 180 °C and then running it through the laminator rollers with a gap width of 100 μ m and a speed of 0.9 m/min. After leaving the laminator, one part of the formed films was immediately dipped into a washing bath containing isopropanol at 25 °C to initiate phase separation due to the action of the non-solvent. The other part of these films was cooled at the air to 25 °C for initiation of the thermal-induced phase separation and then placed into an isopropanol bath to remove the BA. After soaking in this bath for 30 min, both types of films were washed in a second bath with isopropanol to remove residual BA and then air dried at 25 °C.

2.3. Methods

The rheological properties of the PA12/BA solutions were studied on a Discovery HR-2 rotational rheometer (TA Instruments, New Castle, DE, USA) using a cone-plate measuring unit with an angle between the cone and the plate of 2° and a plate diameter of 25 mm. The frequency dependences of the complex viscosity of the solutions were obtained at a constant strain amplitude of 10% in an angular frequency range of 0.628–628 rad/s at 160 °C. The dependence of the dynamic viscosity of the solutions on temperature was obtained at a shear rate of 0.1 s⁻¹ and a cooling rate of 2 °C/min in a temperature range of 160–25 °C. The rheological characteristics were calculated according to the usual equations [84], and the relative error in their determination did not exceed 5%.

The morphology of the surfaces and cross-slices of the porous films were analyzed using a Phenom XL G2 scanning electron microscope (Thermo Fisher Scientific, Breda, The Netherlands) under an accelerating voltage of 15 kV and a pressure of 60 Pa. For the removal of the electric charge, a thin (approximately 5 nm) layer of gold was applied to the samples' surfaces by ion-plasma spraying on a 108 Auto Sputter Coater (Cressington Scientific Instruments, Watford, UK). The surface porosity (φ) of the films was determined by analyzing their SEM images using ImageJ software.

The contact angles of the water droplets on the porous polylactolactam films (θ) were measured by using an LK-1 goniometer (OpenScience, Krasnogorsk, Russia). The films were cut out and placed on an object stage so that the camera captured the image of the interface of the film with a droplet and air. A droplet of distilled water was placed on the sample surface with a dispenser, after which the image was fixed with the camera for subsequent analysis.

The filtration tests were conducted at 25 °C and a pressure of 1 atm in the setup with dead-end cells (active filtration area: approximately 3.14 cm²) equipped with the stirring mechanism. The performance of the polylactolactam membranes was characterized in terms of the permeability coefficient P (kg/m²hbar) and rejection R (%). An aqueous

dispersion of the phthalocyanine particles, with a concentration of 0.01 wt.% and an effective particle diameter of 240 nm, was used as a contaminated test liquid for the microfiltration studies. The relative concentration of phthalocyanine particles in the feed and permeate was evaluated using a UV-vis spectrometer, PE-5400UV (Ecroskhim, Saint Petersburg, Russia), at a wavelength of 600 nm. The permeability coefficient for the pure water and contaminated test liquid was calculated as follows:

$$P = \left(\frac{m}{S\Delta t\Delta p} \right) \cdot h \quad (1)$$

where m is the mass of permeate passed through a membrane with area S in the time interval Δt with a pressure difference Δp (10 atm) and a membrane thickness h .

The rejection was estimated using the following equation:

$$R = \left(1 - \frac{C_p}{C_f} \right) \cdot 100\% \quad (2)$$

where C_p and C_f are the relative particle concentrations in, respectively, the permeate and the feed.

Tensile tests of the PA12 membranes (30 mm length, 5 mm width, and 70–100 μm thick) were performed with a ChemInstruments TT-1100 machine at 25 °C with a constant speed of 3.8 cm/min. The maximum load of the sensor was 11.3 kg.

3. Results

3.1. Theoretical PA12/BA Miscibility

To predict both the solubility of the PA12 in BA and the phase state of their mixtures at different temperatures, it is desirable to be guided by a phase diagram. It can be calculated theoretically from the condition of equality of free-energy increments for each of the mixture components in the coexisting phases [85–87]:

$$\Delta G'_i = \Delta G''_i \quad (3)$$

where $\Delta G'_i$ and $\Delta G''_i$ are the increments of the partial molar free energy of the i -th component in the first and second phases, respectively.

For a two-component mixture, the incremental partial molar free energy can be calculated using the following equation:

$$\Delta G'_1 = RT \left(\ln \varphi_1 + \frac{V_{m,2} - V_{m,1}}{V_{m,2}} \varphi_2 + \chi_{12} \varphi_2^2 \right) \quad (4)$$

where φ_1 and φ_2 are the solvent and polymer volume fractions, respectively; $V_{m,1}$ is the molar volume of the solvent (103.9 cm^3/mol); $V_{m,2}$ is the critical molar volume of the polymer (approximately 4100 cm^3/mol , taking that the critical molecular weight is twice the entanglement molecular weight [88], which was approximately 2000 g/mol for the PA12 [89,90]); R is the universal gas constant; T is the thermodynamic temperature; and χ_{12} is the Flory–Huggins interaction parameter. For the incremental partial molar free energy of the second component, the form of the equation does not change, except that the indices are replaced accordingly.

The Flory–Huggins interaction parameter can be calculated from a weighted arithmetic mean of the three differences between the Hansen solubility parameters of the interacting mixture components [26,91]:

$$\chi_{12} = V_{m,1} \frac{\frac{\delta_{D,1} + \delta_{D,2}}{2} (\delta_{D,1} - \delta_{D,2})^2 + \frac{\delta_{P,1} + \delta_{P,2}}{2} (\delta_{P,1} - \delta_{P,2})^2 + \frac{\delta_{H,1} + \delta_{H,2}}{2} (\delta_{H,1} - \delta_{H,2})^2}{RT \left(\frac{\delta_{D,1} + \delta_{D,2}}{2} + \frac{\delta_{P,1} + \delta_{P,2}}{2} + \frac{\delta_{H,1} + \delta_{H,2}}{2} \right)}, \quad (5)$$

where $\delta_{D,1}$ (18.4 MPa^{0.5}), $\delta_{D,2}$ (17.2 MPa^{0.5}), $\delta_{P,1}$ (6.3 MPa^{0.5}), $\delta_{P,2}$ (4.0 MPa^{0.5}), $\delta_{H,1}$ (13.7 MPa^{0.5}), and $\delta_{H,2}$ (5.1 MPa^{0.5}) are the dispersion, polar, and hydrogen bonding Hansen solubility parameters for the solvent and polymer, respectively [91–93].

Equations (3)–(5) allow for determining the binodal lines, while the spinodal line can be calculated based on the zero value of the second derivative of the free energy on the concentrations of the mixture components [94]:

$$\frac{d^2\Delta G}{d\varphi_1 d\varphi_2} = 0 \quad (6)$$

and the Flory–Huggins equation for free energy [95]:

$$\Delta G = RT \left(\frac{\varphi_1}{V_{m,1}} \ln \varphi_1 + \frac{\varphi_2}{V_{m,2}} \ln \varphi_2 + \chi_{12} \varphi_1 \varphi_2 \right) \quad (7)$$

As a result of combining Equations (6) and (7), the expression for calculating the spinodal line takes the following form:

$$\frac{1}{V_{m,1}\varphi_1} + \frac{1}{V_{m,2}\varphi_2} - 2 \left(\frac{\frac{\delta_{D,1} + \delta_{D,2}}{2} (\delta_{D,1} - \delta_{D,2})^2 + \frac{\delta_{P,1} + \delta_{P,2}}{2} (\delta_{P,1} - \delta_{P,2})^2 + \frac{\delta_{H,1} + \delta_{H,2}}{2} (\delta_{H,1} - \delta_{H,2})^2}{RT \left(\frac{\delta_{D,1} + \delta_{D,2}}{2} + \frac{\delta_{P,1} + \delta_{P,2}}{2} + \frac{\delta_{H,1} + \delta_{H,2}}{2} \right)} \right) = 0 \quad (8)$$

The results of the theoretical calculations of the spinodal and binodal curves are shown in Figure 2. The UCST for the PA12/BA system was 157 °C, and this means that a temperature of 160–180 °C should be sufficient to achieve the complete solubility of PA12 and the subsequent shaping of the resulting solution.

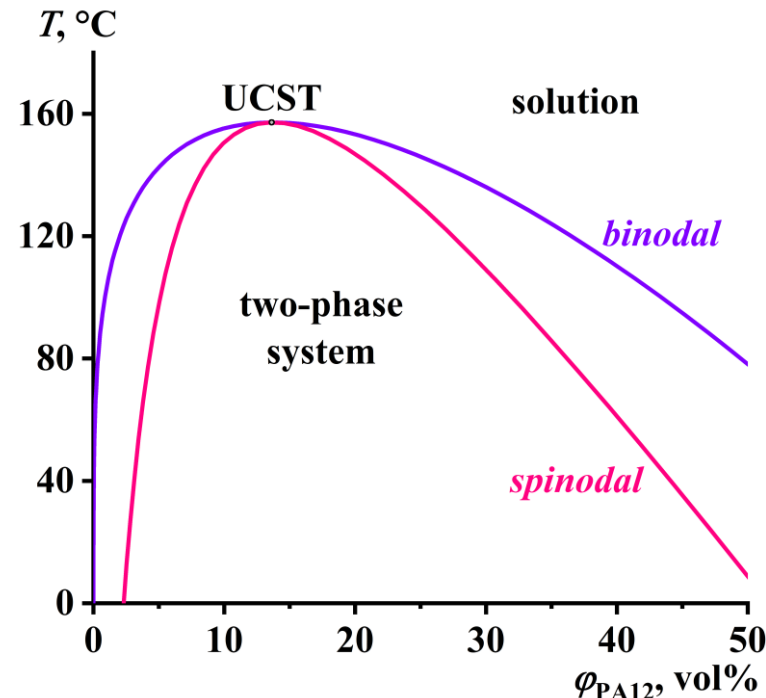


Figure 2. Phase diagram for a mixture of polylaurylactam and benzyl alcohol.

3.2. Viscosimetry of PA12/BA Solutions

The PA12 solutions were Newtonian fluids at 160 °C, like the supercooled melt of this polymer (Figure 3). The absence of non-Newtonian behavior in these systems was probably due to the relatively low molecular weight of the polymer, as a result of which its melt and concentrated solutions contained a small number of macromolecular entanglements.

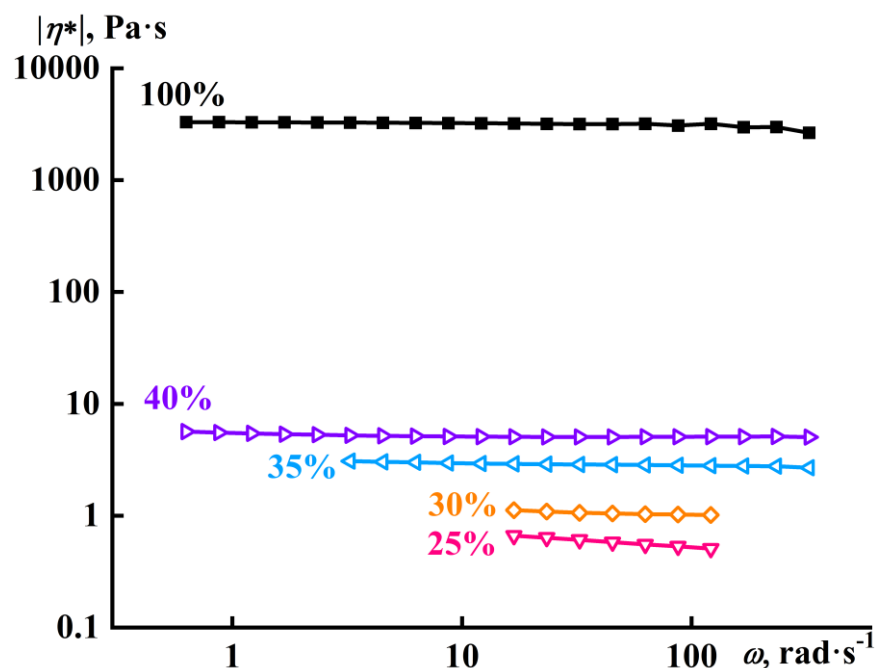


Figure 3. Frequency dependences of the complex viscosity of polylauro lactam solutions in benzyl alcohol at 160 °C. The concentration of polylauro lactam is provided near the curves.

Increasing the concentration of the polyamide expectedly caused an increase in the viscosity, and the concentration dependence of the specific viscosity of the solution was linearized in logarithmic coordinates (Figure 4). In this case, the slope of the straight line is 2.8, i.e., $\eta_{sp} \sim c_{PA12}^{2.8}$. This indicates that all of the solutions under consideration were concentrated rather than dilute, as the viscosity of the latter increased linearly with an increasing polymer concentration [9].

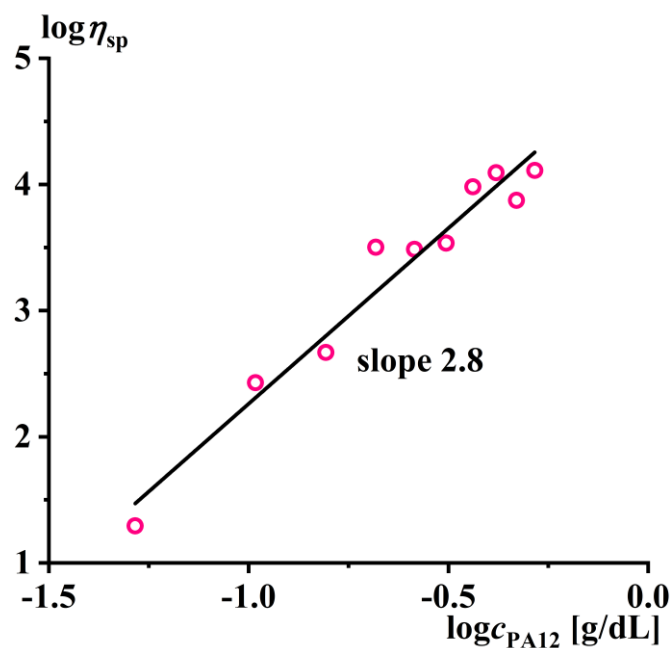


Figure 4. Concentration dependence of the specific viscosity of the polylauro lactam solutions in benzyl alcohol at 160 °C.

As the temperature decreased, the viscosity of both the melt and PA12 solutions gradually decreased until the crystallization point was reached, causing the effective viscosity to rise sharply to an infinitely large value (Figure 5). In the case of the solutions, the onset point of a sharp increase in the viscosity means the moment of their phase separation, i.e., the transition from the liquid homogeneous state to a nominally two-phase system consisting of solvent and semicrystalline polymer. As the polymer concentration decreased, the crystallization temperature shifted toward lower temperatures. This means that BA acted not only as a solvent for PA12 but also as its plasticizer.

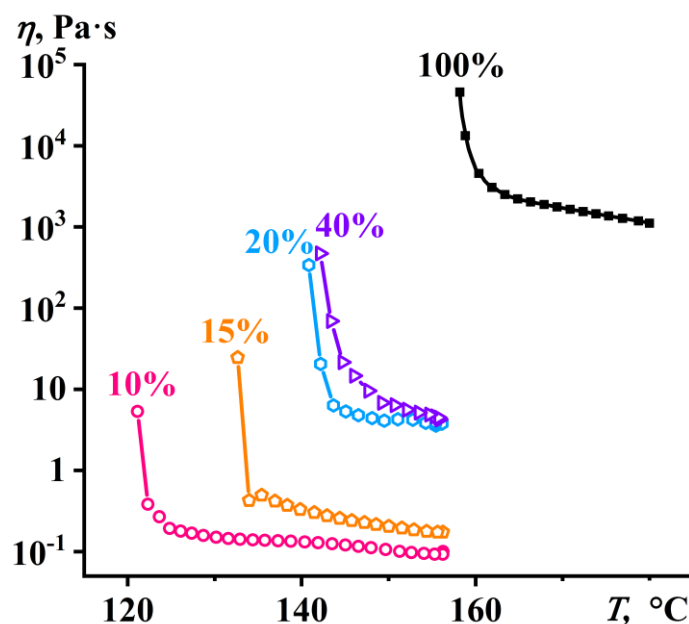


Figure 5. Temperature dependences of the effective viscosity of the polylauro lactam solutions in benzyl alcohol obtained in the cooling mode at a constant shear rate of 0.1 s^{-1} . The concentration of polylauro lactam is provided near the curves.

The depression of the PA12 crystallization temperature can be traced by its dependence on the polymer concentration in the solution (Figure 6). In general, an addition of a large amount of plasticizer to a semicrystalline polymer can cause plasticization of its amorphous part, with an increase in the free volume, leading to the increased mobility of the macromolecular segments and reducing the melting temperature of the polymer and, consequently, its crystallization temperature. In our case, the crystallization of pure PA12 occurred at $158 \text{ }^\circ\text{C}$, while the addition of benzyl alcohol lowered its crystallization temperature. The most pronounced decrease in the temperature took place when the PA12 concentration was reduced to 20% or less.

Thus, the crystallization of the PA12 solutions occurred at temperatures of $121\text{--}142 \text{ }^\circ\text{C}$, while the UCST for the PA12/BA system was $157 \text{ }^\circ\text{C}$ (see Figure 2). Similarly, the pure PA12 crystallized at $158 \text{ }^\circ\text{C}$ (Figure 5), while its melting point was $178 \text{ }^\circ\text{C}$. In this respect, the PA12 melt and solutions were capable of being in a highly supercooled state. Nevertheless, the viscosity of the concentrated solutions, even containing up to 40% PA12, did not exceed $5 \text{ Pa}\cdot\text{s}$. As a result, all of the obtained solutions were very fluid and easily shapeable. At the same time, the preparation and use of more concentrated solutions are technologically unfeasible due to the extremely slow solubility of PA12, difficulty in stirring the PA12/BA mixtures, and their rapid crystallization upon cooling.

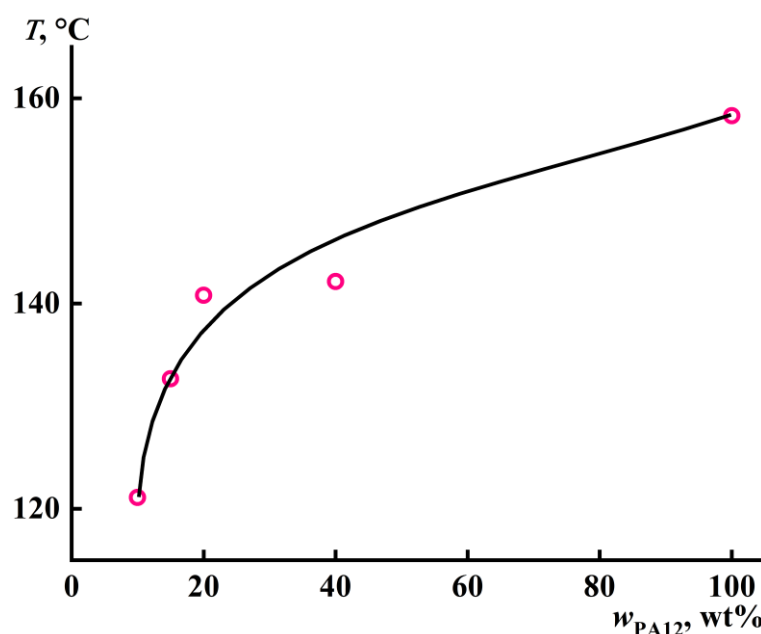


Figure 6. Concentration dependence of the crystallization temperature of the polylauro lactam solution in benzyl alcohol.

3.3. Morphology of the PA12 Films

The easy flowability of the PA12 solutions allows them to be shaped between the two coating anti-adhesion films at elevated temperatures. Then, the resulting hot sandwich film can either be quickly placed in a bath containing a non-solvent with the subsequent removal of the coating films or cooled in the air for phase separation due to the PA12's crystallization. Non-solvent-induced phase separation occurs due to the enrichment of the polymer solution with a non-solvent and the resulting loss of solubility of the polymer with the formation of a two-phase system [97]. As a result, a porous film is formed from the amorphous polymer-enriched phase, the pores of which represent the polymer-depleted phase. Then the amorphous polymer-enriched phase partially crystallizes because of the temperature decrease. Phase separation under the influence of air occurs due to the cooling of the polymer solution, causing partial crystallization of the polymer with the formation of a two-phase system [98]. As a result, the crystallizing polymer forms a porous film whose pores are filled with solvent. Thus, the difference between the two types of phase separation is the initial phase state of the polymeric phase—amorphous or semicrystalline. In turn, this leads to differences in the kinetics of phase separation and different sizes of formed pores due to the different relaxation rates of the amorphous and semicrystalline polymeric phases [31].

When films are obtained by cooling a relatively low-concentrated solution containing 25% PA12, a low-dense structure is formed, consisting of weakly bonded individual polymer spherical aggregates (Figure 7a,b). In this case, during the cooling and phase separation of the solution, the role of the continuous phase was played most likely by a dilute PA12/BA solution, which was then removed by washing the resulting film in isopropanol. In turn, a PA12-rich crystallizing phase formed due to the phase separation is transformed into dispersed spherical-shaped polymer particles. The result is the formation of a brittle film unsuitable as a membrane material. A formation of this type of morphology is due to the low concentration of the polymer in the solution, which results in the absence of macromolecular entanglements; otherwise, the concentrated polymer solution would form a gel [99]. Previously, thermally induced phase separation of the dilute polymer solutions was applied to obtain polymer microspheres and nanoparticles of the different structures [100–103].

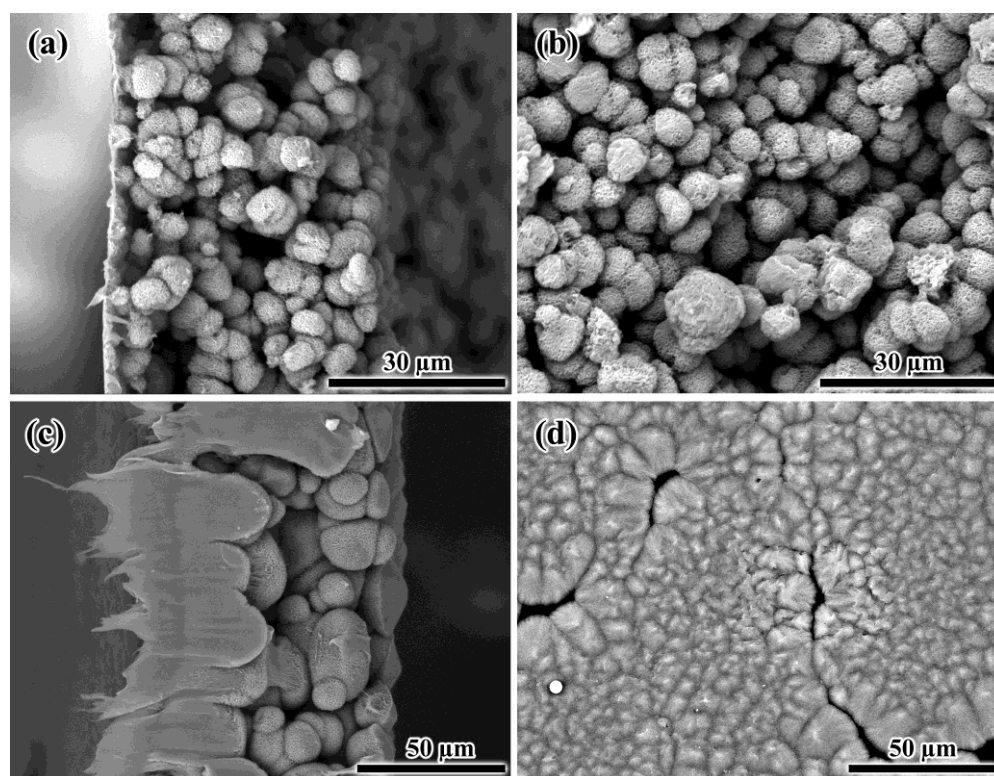


Figure 7. SEM images of the cross-sections (a,c) and surfaces (b,d) of the porous films obtained from 25% (a,b) and 40% (c,d) poly(lauro)lactam solutions by cooling.

When using a highly concentrated solution containing 40% PA12, the size of the formed polymer aggregates increased, while the film surface became much denser but contained pores (Figure 7c,d). In this respect, the polymer still formed a dispersed phase as a result of the phase separation of the solution under cooling despite its high concentration. This was confirmed by a closer look at the spherical polymer aggregates, which resembled corals or sponges interconnected by filamentous formations in some cases (Figure 8). This structure of the aggregates allowed for assuming their porosity. However, one cannot accurately assess how well the porosity is formed in the depths of large aggregates, which may have no pores in the inner layers.

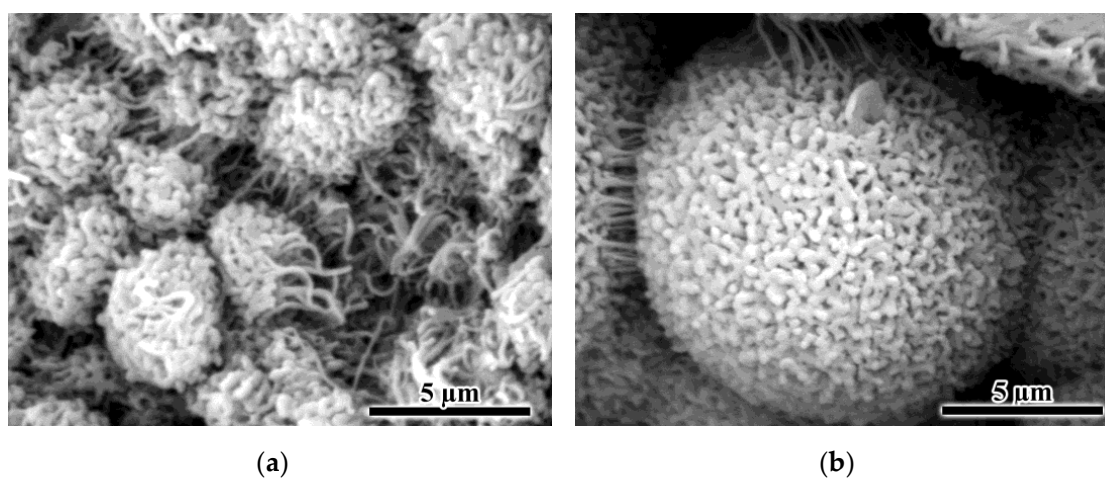


Figure 8. SEM images of aggregates obtained from 25% (a) and 40% (b) poly(lauro)lactam solutions by cooling.

In the case of obtaining films by the precipitation of 20–30% solutions, BA is replaced by the non-solvent—*isopropanol*. As a result, phase separation occurs more successfully in terms of obtaining the membrane material. In this case, the continuous phase was formed from the PA12-rich solution, while the dispersed phase was a dilute polymer solution, after the removal of which sinuous pores remained in the film volume (Figure 9a,c). When the 20% PA12 solution was used, the surface of the films was formed by large, irregularly shaped aggregates with cracks between them (Figure 9b). The use of the 30% solution reduced the size of the surface aggregates, having small holes between themselves rather than cracks (Figure 9d). Thus, it can be assumed that in the case of a less concentrated solution, there is a strong shrinkage of the obtained film, and this leads to the formation of surface cracks.

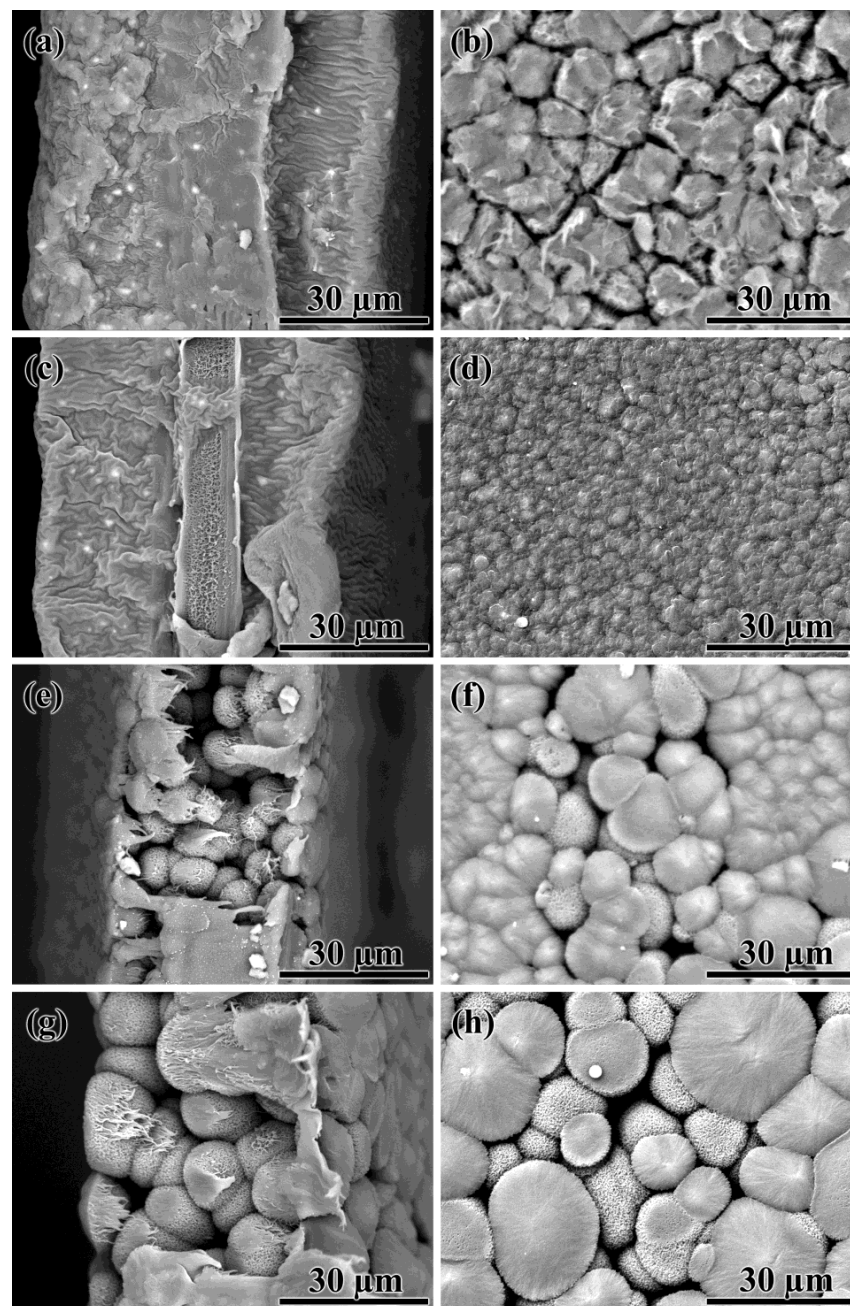


Figure 9. SEM images of the cross-sections (a,c,e,g) and surfaces (b,d,f,h) of the porous films obtained from 20% (a,b), 30% (c,d), 35% (e,f), and 40% (g,h) poly(lauro)lactam solutions by its precipitation with *isopropanol*.

Interestingly, one can detect a pronounced central layer in the core of the film obtained from a more concentrated 30% solution (Figure 9c). Within this layer, filament pores also formed (Figure 10a). Perhaps the outer layers of the forming film cool down and harden quickly due to the higher polymer concentration and the large temperature difference between the solution (180 °C) and the non-solvent (25 °C), slowing down the diffusion rate of the non-solvent deep into the film. In this case, local phase separation may occur in the center of the film due to the cooling of the solution rather than the action of the non-solvent. This was confirmed by the similarity in the filamentary structures of the film core (Figure 10a) and spherical aggregates (Figure 8a) formed during phase separation initiated by cooling. In contrast, the pores within the film edges had a sinuous shape, and the surface of the film cross-section resembled that of a mammalian brain (Figure 10b). In this respect, the formed film can be considered an asymmetric membrane.

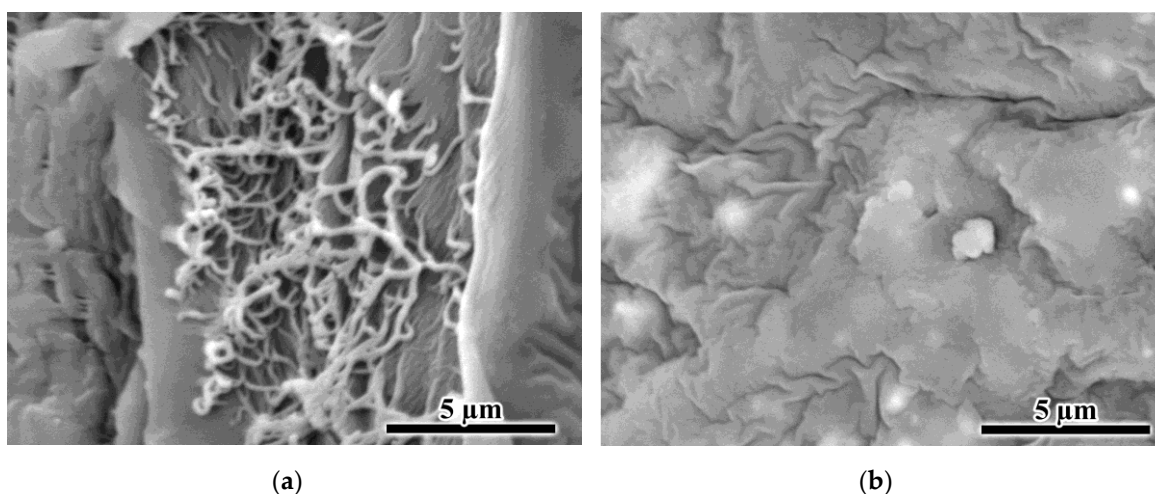


Figure 10. SEM images of the porous formations in the center (a) and at the edges (b) of the film obtained from the 30% polylauro lactam solution by precipitation with isopropanol.

A higher PA12 concentration of 35–40% led to the fact that the phase separation occurred due to the cooling by cold non-solvent rather than its diffusion into the forming film. The morphology of the surfaces and cross-sections of the resulting films (Figure 9e–h) resembled that of the films obtained by thermal-induced phase separation (see Figure 7). It can be assumed that a high polymer concentration slows down the diffusion of the non-solvent into the polymer solution because of either its higher viscosity or a denser skin that forms on its surface upon contact with the non-solvent.

Thus, 20–30% PA12 solutions are more suitable for obtaining membranes in terms of the morphology of the resulting films. In this case, the phase separation should be initiated by exposure to a non-solvent rather than a decrease in temperature. At this relatively low polymer concentration, there is probably a rapid diffusion of BA from the solution into the non-solvent, causing a dramatic increase in the polymer concentration in the solution. Therefore, the subsequent phase separation occurs with the formation of a continuous medium from the polymer rather than from the non-solvent. In contrast, the initially higher polymer concentration in the 35–40% solutions is insufficient to form a continuous medium from the polymer. It is because the diffusion between the non-solvent and concentrated solution occurs slowly without a noticeable change in the polymer concentration in the solution, leading to phase separation with the formation of a continuous medium from the polymer-poor phase.

3.4. PA12 Porous Films as Microfiltration Membranes

Let us consider the application of porous films as microfiltration membranes using the example of three specimens obtained from solutions containing different amounts of

PA12 and in which the phase separation was initiated by two different methods. The film produced from the 40% solution upon cooling rejects poorly submicron phthalocyanine particles with an average size of 240 nm; the rejection is as low as 58.4% ($R_{240\text{nm}}$, Table 1). This is most likely due to the presence of large cracks on the surface of this film (see Figure 7d). This sample was also quite brittle and had a low tensile strength of approximately 0.6 MPa. At the same time, it does not have high water permeability despite the cracks, indicating a small internal porosity, i.e., the measured permeate flow is due to the presence of defects rather than pores. This conclusion also is confirmed by the low surface porosity (9.1%, Table 1) and the fact that the water contact angle for this sample ($87^\circ \pm 10^\circ$) was comparable to that for nonporous polylactolactam ($92^\circ \pm 3^\circ$).

Table 1. Porosity, wettability, permeability, microfiltration ability, and tensile strength of the porous films from polylactolactam.

Polymer Content	40% PA12	40% PA12	30% PA12
Phase separation	temperature induced	non-solvent induced	non-solvent induced
ϕ , %	9.1	12.4	22.8
θ , °	87 ± 10	73 ± 1	71 ± 4
P_{water} , kg/m ² hbar	2.1	142	69.9
$P_{\text{dispersion}}$, kg/m ² hbar	4.7	1.0	1.5
$R_{240\text{nm}}$, %	58.4	98.9	99.6
τ , MPa	0.6 ± 0.1	1.8 ± 0.6	1.9 ± 0.3

The action of the non-solvent on the same 40% solution led to a porous film with quite different physicochemical and transport characteristics. The resulting film had three times higher strength and rejected 98.9% of the phthalocyanine particles (Table 1). In addition, the film had a 68 times higher pure-water permeability (P_{water}), indicating its better porosity. The higher porosity also is confirmed by the calculated surface porosity, which was higher (12.4% versus 9.1%), and the better wettability of the film with water (73° versus 87°). This improvement in the wettability with the increasing porosity is explained by the Wenzel model [104], according to which the wettability of hydrophobic materials deteriorates with increasing porosity while that of hydrophilic materials conversely increases. Thus, compared to temperature-induced phase separation, the non-solvent-induced phase separation provided the membrane with higher roughness (in concurrence with the SEM data, see Figures 7d and 9h) and better wetting due to the relative hydrophilicity of PA12. In this case, the filtration of the aqueous phthalocyanine dispersion resulted in more than a 100 times lower permeability than that of pure water. This may be due to the clogging of pores with phthalocyanine particles.

The decrease in the polyamide concentration to 30% with the non-solvent-induced formation of a porous film yielded the least defective membrane according to the SEM data (see Figure 9d). Indeed, this film had the highest strength (1.9 MPa, Table 1) and the best rejection of the phthalocyanine particles (99.6%). In addition, the film had the highest surface porosity (22.8%), good wettability (71°), and an acceptable filtration rate of the phthalocyanine dispersion (1.5 kg/m²hbar).

The final question concerns the performance of the obtained microfiltration membrane compared to membranes from other polymers. The correct conditions for a comparison are the same unfiltered fluid and a polymer having a comparable chemical resistance, which means the same challenges in forming membranes from it. Suitable references are microfiltration membranes made from polymethylpentene (PMP). The best-quality PMP membrane has the same high rejection coefficient of 99% for the same aqueous dispersion of phthalocyanine particles [64]. However, the PMP membrane is dozens of times less permeable to water than the PA12 membrane (1.9 kg/m²hbar versus 69.9 kg/m²hbar) but has five times higher tensile strength (9.1 MPa versus 1.9 MPa). In other words, the PA12 membranes are more porous, which allows for faster filtration but at the cost of reduced mechanical strength.

4. Conclusions

The novelty of this work consists of obtaining membranes from polylauro lactam using its solutions in benzyl alcohol, which is a green alternative to the expensive fluorinated or toxic phenolic solvents of this polymer. For the first time, the non-solvent- and temperature-induced methods allowed for parallel-making microfiltration membranes from this polymer for a direct comparison of the effectiveness of these methods and the performance of the resultant membranes. Hot solutions of polylauro lactam in benzyl alcohol are suitable for obtaining porous films. These solutions have low viscosity and undergo phase separation due to the crystallization of polylauro lactam when cooling below 120–140 °C. However, this temperature-induced phase separation does not allow for obtaining nonbrittle films suitable as membranes, since the resulting polymer-enriched phase forms dispersed particles rather than a continuous medium. This situation can be fundamentally reversed if the phase separation is initiated by the action of a non-solvent, such as isopropanol. If the polymer concentration in the phase-separating solution does not exceed 30%, polylauro lactam forms a continuous phase that contains sinuous micron-sized pores. The resulting material can be shaped in the form of thin films that can be considered chemical-resistant membranes for microfiltration. A study of the transport properties of the non-solvent-induced phase-separated film from a 30% solution revealed its ability to reject 99.6% of the 240 nm particles at a filtration rate of 1.5 kg/m²hbar.

Author Contributions: Conceptualization, S.O.I. (Sergey O. Ilyin); methodology, S.O.I. (Sergey O. Ilyin) and T.S.A.; formal analysis, S.O.I. (Sergey O. Ilyin), T.S.A., and S.O.I. (Svetlana O. Ilyina); investigation, S.O.I. (Svetlana O. Ilyina), T.S.A. and S.O.I. (Sergey O. Ilyin); writing—original draft preparation, S.O.I. (Svetlana O. Ilyina); writing—review and editing, S.O.I. (Sergey O. Ilyin); visualization, S.O.I. (Svetlana O. Ilyina); project administration, S.O.I. (Sergey O. Ilyin). All authors have read and agreed to the published version of the manuscript.

Funding: This research received no external funding.

Institutional Review Board Statement: Not applicable.

Informed Consent Statement: Not applicable.

Data Availability Statement: The data presented in this study are available upon request from the corresponding author.

Acknowledgments: The SEM images were obtained in the Shared Research Center “Analytical Center of Deep Oil Processing and Petrochemistry of TIPS RAS”. This research was carried out within the State Program of A.V. Topchiev Institute of Petrochemical Synthesis.

Conflicts of Interest: The authors declare no conflict of interest.

References

1. Takht Ravanchi, M.; Kaghazchi, T.; Kargari, A. Application of Membrane Separation Processes in Petrochemical Industry: A Review. *Desalination* **2009**, *235*, 199–244. [[CrossRef](#)]
2. Iulianelli, A.; Drioli, E. Membrane Engineering: Latest Advancements in Gas Separation and Pre-Treatment Processes, Petrochemical Industry and Refinery, and Future Perspectives in Emerging Applications. *Fuel Process. Technol.* **2020**, *206*, 106464. [[CrossRef](#)]
3. Yang, Z.; Zhou, Y.; Feng, Z.; Rui, X.; Zhang, T.; Zhang, Z. A Review on Reverse Osmosis and Nanofiltration Membranes for Water Purification. *Polymers* **2019**, *11*, 1252. [[CrossRef](#)]
4. Pangarkar, B.L.; Deshmukh, S.K.; Sapkal, V.S.; Sapkal, R.S. Review of Membrane Distillation Process for Water Purification. *Desalin. Water Treat.* **2016**, *57*, 2959–2981. [[CrossRef](#)]
5. Bernardo, P.; Drioli, E.; Golemme, G. Membrane Gas Separation: A Review/State of the Art. *Ind. Eng. Chem. Res.* **2009**, *48*, 4638–4663. [[CrossRef](#)]
6. Ismail, A.F.; Khulbe, K.C.; Matsuura, T. Gas Separation Membrane Materials and Structures. In *Gas Separation Membranes: Polymeric and Inorganic*; Ismail, A.F., Chandra Khulbe, K., Matsuura, T., Eds.; Springer International Publishing: Cham, Switzerland, 2015; pp. 37–192. ISBN 978-3-319-01095-3.
7. Silva, S.S.; Popa, E.G.; Gomes, M.E.; Cerqueira, M.; Marques, A.P.; Caridade, S.G.; Teixeira, P.; Sousa, C.; Mano, J.F.; Reis, R.L. An Investigation of the Potential Application of Chitosan/Aloe-Based Membranes for Regenerative Medicine. *Acta Biomater.* **2013**, *9*, 6790–6797. [[CrossRef](#)]

8. Lim, R. Concise Review: Fetal Membranes in Regenerative Medicine: New Tricks from an Old Dog? *Stem Cells Transl. Med.* **2017**, *6*, 1767–1776. [[CrossRef](#)]
9. Mollahosseini, A.; Abdelrasoul, A.; Shoker, A. A Critical Review of Recent Advances in Hemodialysis Membranes Hemocompatibility and Guidelines for Future Development. *Mater. Chem. Phys.* **2020**, *248*, 122911. [[CrossRef](#)]
10. Said, N.; Lau, W.J.; Ho, Y.-C.; Lim, S.K.; Abidin, M.N.Z.; Ismail, A.F. A Review of Commercial Developments and Recent Laboratory Research of Dialyzers and Membranes for Hemodialysis Application. *Membranes* **2021**, *11*, 767. [[CrossRef](#)]
11. Dahiya, D.; Kumar, M.; Pugazhenthii, G.; Vasanth, D. Separation of Bacteria *Kocuria Rhizophila* from Fermentation Broth by Cross-Flow Microfiltration Using Inexpensive Tubular Ceramic Membrane. *Arab. J. Sci. Eng.* **2022**, *47*, 5767–5776. [[CrossRef](#)]
12. Tomczak, W.; Gryta, M. Cross-Flow Microfiltration of Glycerol Fermentation Broths with *Citrobacter Freundii*. *Membranes* **2020**, *10*, 67. [[CrossRef](#)]
13. Ulbricht, M. Advanced Functional Polymer Membranes. *Polymer* **2006**, *47*, 2217–2262. [[CrossRef](#)]
14. Lin, Y.S.; Kumakiri, I.; Nair, B.N.; Alsyouri, H. Microporous Inorganic Membranes. *Sep. Purif. Methods* **2002**, *31*, 229–379. [[CrossRef](#)]
15. Verweij, H. Inorganic Membranes. *Curr. Opin. Chem. Eng.* **2012**, *1*, 156–162. [[CrossRef](#)]
16. Wang, J.; Dlamini, D.S.; Mishra, A.K.; Pendergast, M.T.M.; Wong, M.C.Y.; Mamba, B.B.; Freger, V.; Verliefde, A.R.D.; Hoek, E.M.V. A Critical Review of Transport through Osmotic Membranes. *J. Membr. Sci.* **2014**, *454*, 516–537. [[CrossRef](#)]
17. Pinnau, I.; Freeman, B.D. Formation and Modification of Polymeric Membranes: Overview. In *Membrane Formation and Modification*; ACS Symposium Series; American Chemical Society: Washington, DC, USA, 1999; Volume 744, pp. 1–22. ISBN 978-0-8412-3604-2.
18. Cot, L.; Ayrat, A.; Durand, J.; Guizard, C.; Hovnanian, N.; Julbe, A.; Larbot, A. Inorganic Membranes and Solid State Sciences. *Solid State Sci.* **2000**, *2*, 313–334. [[CrossRef](#)]
19. Jiang, S.; Li, Y.; Ladewig, B.P. A Review of Reverse Osmosis Membrane Fouling and Control Strategies. *Sci. Total Environ.* **2017**, *595*, 567–583. [[CrossRef](#)]
20. Tomczak, W.; Gryta, M. Comparison of Polypropylene and Ceramic Microfiltration Membranes Applied for Separation of 1,3-PD Fermentation Broths and *Saccharomyces Cerevisiae* Yeast Suspensions. *Membranes* **2021**, *11*, 44. [[CrossRef](#)]
21. Alresheedi, M.T.; Barbeau, B.; Basu, O.D. Comparisons of NOM Fouling and Cleaning of Ceramic and Polymeric Membranes during Water Treatment. *Sep. Purif. Technol.* **2019**, *209*, 452–460. [[CrossRef](#)]
22. Wen, Q.; Di, J.; Zhao, Y.; Wang, Y.; Jiang, L.; Yu, J. Flexible Inorganic Nanofibrous Membranes with Hierarchical Porosity for Efficient Water Purification. *Chem. Sci.* **2013**, *4*, 4378–4382. [[CrossRef](#)]
23. Fard, A.K.; McKay, G.; Buekenhoudt, A.; Al Sulaiti, H.; Motmans, F.; Khraishah, M.; Atieh, M. Inorganic Membranes: Preparation and Application for Water Treatment and Desalination. *Materials* **2018**, *11*, 74. [[CrossRef](#)] [[PubMed](#)]
24. Liu, H.; Hsieh, Y.-L. Ultrafine Fibrous Cellulose Membranes from Electrospinning of Cellulose Acetate. *J. Polym. Sci. Part B Polym. Phys.* **2002**, *40*, 2119–2129. [[CrossRef](#)]
25. Sukma, F.M.; Çulfaz-Emecen, P.Z. Cellulose Membranes for Organic Solvent Nanofiltration. *J. Membr. Sci.* **2018**, *545*, 329–336. [[CrossRef](#)]
26. Ilyin, S.O.; Makarova, V.V.; Anokhina, T.S.; Ignatenko, V.Y.; Brantseva, T.V.; Volkov, A.V.; Antonov, S.V. Diffusion and Phase Separation at the Morphology Formation of Cellulose Membranes by Regeneration from N-Methylmorpholine N-Oxide Solutions. *Cellulose* **2018**, *25*, 2515–2530. [[CrossRef](#)]
27. Sokolnicki, A.M.; Fisher, R.J.; Harrah, T.P.; Kaplan, D.L. Permeability of Bacterial Cellulose Membranes. *J. Membr. Sci.* **2006**, *272*, 15–27. [[CrossRef](#)]
28. Jung, R.; Kim, Y.; Kim, H.-S.; Jin, H.-J. Antimicrobial Properties of Hydrated Cellulose Membranes with Silver Nanoparticles. *J. Biomater. Sci. Polym. Ed.* **2009**, *20*, 311–324. [[CrossRef](#)]
29. Evans, B.R.; O’Neill, H.M.; Malyvanh, V.P.; Lee, I.; Woodward, J. Palladium-Bacterial Cellulose Membranes for Fuel Cells. *Biosens. Bioelectron.* **2003**, *18*, 917–923. [[CrossRef](#)]
30. Barud, H.S.; Barrios, C.; Regiani, T.; Marques, R.F.C.; Verelst, M.; Dexpert-Ghys, J.; Messaddeq, Y.; Ribeiro, S.J.L. Self-Supported Silver Nanoparticles Containing Bacterial Cellulose Membranes. *Mater. Sci. Eng. C* **2008**, *28*, 515–518. [[CrossRef](#)]
31. Tang, Y.; Lin, Y.; Ford, D.M.; Qian, X.; Cervellere, M.R.; Millett, P.C.; Wang, X. A Review on Models and Simulations of Membrane Formation via Phase Inversion Processes. *J. Membr. Sci.* **2021**, *640*, 119810. [[CrossRef](#)]
32. Wang, J.; Yue, Z.; Ince, J.S.; Economy, J. Preparation of Nanofiltration Membranes from Polyacrylonitrile Ultrafiltration Membranes. *J. Membr. Sci.* **2006**, *286*, 333–341. [[CrossRef](#)]
33. Scharnagl, N.; Buschatz, H. Polyacrylonitrile (PAN) Membranes for Ultra- and Microfiltration. *Desalination* **2001**, *139*, 191–198. [[CrossRef](#)]
34. Zhao, C.; Xue, J.; Ran, F.; Sun, S. Modification of Polyethersulfone Membranes—A Review of Methods. *Prog. Mater. Sci.* **2013**, *58*, 76–150. [[CrossRef](#)]
35. Park, H.C.; Kim, Y.P.; Kim, H.Y.; Kang, Y.S. Membrane Formation by Water Vapor Induced Phase Inversion. *J. Membr. Sci.* **1999**, *156*, 169–178. [[CrossRef](#)]
36. Tan, X.; Rodrigue, D. A Review on Porous Polymeric Membrane Preparation. Part I: Production Techniques with Polysulfone and Poly (Vinylidene Fluoride). *Polymers* **2019**, *11*, 1160. [[CrossRef](#)] [[PubMed](#)]
37. Tan, X.; Rodrigue, D. A Review on Porous Polymeric Membrane Preparation. Part II: Production Techniques with Polyethylene, Polydimethylsiloxane, Polypropylene, Polyimide, and Polytetrafluoroethylene. *Polymers* **2019**, *11*, 1310. [[CrossRef](#)] [[PubMed](#)]

38. Stucki, M.; Loepfe, M.; Stark, W.J. Porous Polymer Membranes by Hard Templating—A Review. *Adv. Eng. Mater.* **2018**, *20*, 1700611. [[CrossRef](#)]
39. Kimmerle, K.; Strathmann, H. Analysis of the Structure-Determining Process of Phase Inversion Membranes. *Desalination* **1990**, *79*, 283–302. [[CrossRef](#)]
40. Ilyin, S.O.; Makarova, V.V.; Anokhina, T.S.; Volkov, A.V.; Antonov, S.V. Effect of Coagulating Agent Viscosity on the Kinetics of Formation, Morphology, and Transport Properties of Cellulose Nanofiltration Membranes. *Polym. Sci. Ser. A* **2017**, *59*, 676–684. [[CrossRef](#)]
41. Cheng, L.-P.; Lin, D.-J.; Shih, C.-H.; Dwan, A.-H.; Gryte, C.C. PVDF Membrane Formation by Diffusion-Induced Phase Separation—Morphology Prediction Based on Phase Behavior and Mass Transfer Modeling. *J. Polym. Sci. Part B Polym. Phys.* **1999**, *37*, 2079–2092. [[CrossRef](#)]
42. Rozelle, L.; Cadotte, J.E.; Corneliussen, R.D.; Erickson, E.E.; Cobian, K.E.; Kopp, C.V., Jr. Phase Inversion Membranes. In *Encyclopedia of Separation Science*; Mulder, M., Ed.; Academic Press: Cambridge, MA, USA, 2000; pp. 3331–3346.
43. Perepechkin, L.P. Methods for Obtaining Polymeric Membranes. *Russ. Chem. Rev.* **1988**, *57*, 539–548. [[CrossRef](#)]
44. Radjabian, M.; Abetz, V. Advanced Porous Polymer Membranes from Self-Assembling Block Copolymers. *Prog. Polym. Sci.* **2020**, *102*, 101219. [[CrossRef](#)]
45. Guillen, G.R.; Pan, Y.; Li, M.; Hoek, E.M.V. Preparation and Characterization of Membranes Formed by Nonsolvent Induced Phase Separation: A Review. *Ind. Eng. Chem. Res.* **2011**, *50*, 3798–3817. [[CrossRef](#)]
46. Wang, D.-M.; Lai, J.-Y. Recent Advances in Preparation and Morphology Control of Polymeric Membranes Formed by Nonsolvent Induced Phase Separation. *Curr. Opin. Chem. Eng.* **2013**, *2*, 229–237. [[CrossRef](#)]
47. Anokhina, T.S.; Ignatenko, V.Y.; Kostyuk, A.V.; Ilyin, S.O.; Volkov, A.V.; Antonov, S.V. The Effect of the Nature of a Coagulant on the Nanofiltration Properties of Cellulose Membranes Formed from Solutions in Ionic Media. *Membr. Membr. Technol.* **2020**, *2*, 149–158. [[CrossRef](#)]
48. Ashtiani, S.; Khoshnamvand, M.; Číhal, P.; Dendisová, M.; Randová, A.; Bouša, D.; Shaliutina-Kolešová, A.; Sofer, Z.; Friess, K. Fabrication of a PVDF Membrane with Tailored Morphology and Properties via Exploring and Computing Its Ternary Phase Diagram for Wastewater Treatment and Gas Separation Applications. *RSC Adv.* **2020**, *10*, 40373–40383. [[CrossRef](#)] [[PubMed](#)]
49. Pervin, R.; Ghosh, P.; Basavaraj, M.G. Tailoring Pore Distribution in Polymer Films via Evaporation Induced Phase Separation. *RSC Adv.* **2019**, *9*, 15593–15605. [[CrossRef](#)] [[PubMed](#)]
50. Matsuyama, H.; Teramoto, M.; Nakatani, R.; Maki, T. Membrane Formation via Phase Separation Induced by Penetration of Nonsolvent from Vapor Phase. II. Membrane Morphology. *J. Appl. Polym. Sci.* **1999**, *74*, 171–178. [[CrossRef](#)]
51. Venault, A.; Chang, Y.; Wang, D.-M.; Bouyer, D. A Review on Polymeric Membranes and Hydrogels Prepared by Vapor-Induced Phase Separation Process. *Polym. Rev.* **2013**, *53*, 568–626. [[CrossRef](#)]
52. Kim, J.F.; Kim, J.H.; Lee, Y.M.; Drioli, E. Thermally Induced Phase Separation and Electrospinning Methods for Emerging Membrane Applications: A Review. *AIChE J.* **2016**, *62*, 461–490. [[CrossRef](#)]
53. Jung, J.T.; Kim, J.F.; Wang, H.H.; di Nicolo, E.; Drioli, E.; Lee, Y.M. Understanding the Non-Solvent Induced Phase Separation (NIPS) Effect during the Fabrication of Microporous PVDF Membranes via Thermally Induced Phase Separation (TIPS). *J. Membr. Sci.* **2016**, *514*, 250–263. [[CrossRef](#)]
54. Ignatenko, V.Y.; Anokhina, T.S.; Ilyin, S.O.; Kostyuk, A.V.; Bakhtin, D.S.; Makarova, V.V.; Antonov, S.V.; Volkov, A.V. Phase Separation of Polymethylpentene Solutions for Producing Microfiltration Membranes. *Polym. Sci. Ser. A* **2020**, *62*, 292–299. [[CrossRef](#)]
55. Dong, X.; Lu, D.; Harris, T.A.L.; Escobar, I.C. Polymers and Solvents Used in Membrane Fabrication: A Review Focusing on Sustainable Membrane Development. *Membranes* **2021**, *11*, 309. [[CrossRef](#)] [[PubMed](#)]
56. Lloyd, D.R.; Kinzer, K.E.; Tseng, H.S. Microporous Membrane Formation via Thermally Induced Phase Separation. I. Solid-Liquid Phase Separation. *J. Membr. Sci.* **1990**, *52*, 239–261. [[CrossRef](#)]
57. Lloyd, D.R.; Kim, S.S.; Kinzer, K.E. Microporous Membrane Formation via Thermally-Induced Phase Separation. II. Liquid—Liquid Phase Separation. *J. Membr. Sci.* **1991**, *64*, 1–11. [[CrossRef](#)]
58. Pasman, T.; Baptista, D.; van Riet, S.; Truckenmüller, R.K.; Hiemstra, P.S.; Rottier, R.J.; Stamatalis, D.; Poot, A.A. Development of Porous and Flexible PTMC Membranes for In Vitro Organ Models Fabricated by Evaporation-Induced Phase Separation. *Membranes* **2020**, *10*, 330. [[CrossRef](#)] [[PubMed](#)]
59. Habib, S.; Weinman, S.T. A Review on the Synthesis of Fully Aromatic Polyamide Reverse Osmosis Membranes. *Desalination* **2021**, *502*, 114939. [[CrossRef](#)]
60. Guan, K.; Zhang, L.; Wang, S.; Takagi, R.; Matsuyama, H. Controlling the Formation of Porous Polyketone Membranes via a Cross-Linkable Alginate Additive for Oil-in-Water Emulsion Separations. *J. Membr. Sci.* **2020**, *611*, 118362. [[CrossRef](#)]
61. Khayet, M.; Matsuura, T. Preparation and Characterization of Polyvinylidene Fluoride Membranes for Membrane Distillation. *Ind. Eng. Chem. Res.* **2001**, *40*, 5710–5718. [[CrossRef](#)]
62. Huang, Q.-L.; Xiao, C.; Feng, X.; Hu, X.-Y. Design of Super-Hydrophobic Microporous Polytetrafluoroethylene Membranes. *New J. Chem.* **2013**, *37*, 373–379. [[CrossRef](#)]
63. Ignatenko, V.Y.; Anokhina, T.S.; Ilyin, S.O.; Kostyuk, A.V.; Bakhtin, D.S.; Antonov, S.V.; Volkov, A.V. Fabrication of Microfiltration Membranes from Polyisobutylene/Polymethylpentene Blends. *Polym. Int.* **2020**, *69*, 165–172. [[CrossRef](#)]

64. Ilyin, S.; Ignatenko, V.; Anokhina, T.; Bakhtin, D.; Kostyuk, A.; Dmitrieva, E.; Antonov, S.; Volkov, A. Formation of Microfiltration Membranes from PMP/PIB Blends: Effect of PIB Molecular Weight on Membrane Properties. *Membranes* **2020**, *10*, 9. [[CrossRef](#)] [[PubMed](#)]
65. Huang, L.; McCutcheon, J.R. Hydrophilic Nylon 6,6 Nanofibers Supported Thin Film Composite Membranes for Engineered Osmosis. *J. Membr. Sci.* **2014**, *457*, 162–169. [[CrossRef](#)]
66. Huang, L.; Bui, N.-N.; Meyering, M.T.; Hamlin, T.J.; McCutcheon, J.R. Novel Hydrophilic Nylon 6,6 Microfiltration Membrane Supported Thin Film Composite Membranes for Engineered Osmosis. *J. Membr. Sci.* **2013**, *437*, 141–149. [[CrossRef](#)]
67. Li, Y.L.; Hao, X.M.; Guo, Y.F.; Chen, X.; Yang, Y.; Wang, J.M. Study on the Acid Resistant Properties of Bio-Based Nylon 56 Fiber Compared with the Fiber of Nylon 6 and Nylon 66. *Adv. Mater. Res.* **2014**, *1048*, 57–61. [[CrossRef](#)]
68. Martino, L.; Basilissi, L.; Farina, H.; Ortenzi, M.A.; Zini, E.; Di Silvestro, G.; Scandola, M. Bio-Based Polyamide 11: Synthesis, Rheology and Solid-State Properties of Star Structures. *Eur. Polym. J.* **2014**, *59*, 69–77. [[CrossRef](#)]
69. Ahsan, M.M.; Jeon, H.; Nadarajan, S.P.; Chung, T.; Yoo, H.-W.; Kim, B.-G.; Patil, M.D.; Yun, H. Biosynthesis of the Nylon 12 Monomer, ω -Aminododecanoic Acid with Novel CYP153A, AlkI, and ω -TA Enzymes. *Biotechnol. J.* **2018**, *13*, 1700562. [[CrossRef](#)]
70. Stephens, J.S.; Chase, D.B.; Rabolt, J.F. Effect of the Electrospinning Process on Polymer Crystallization Chain Conformation in Nylon-6 and Nylon-12. *Macromolecules* **2004**, *37*, 877–881. [[CrossRef](#)]
71. Fina, L.J.; Yu, H.H. Fermi Resonance in the Infrared Spectra of Nylon-11. *J. Polym. Sci. Part B Polym. Phys.* **1992**, *30*, 1073–1080. [[CrossRef](#)]
72. Lánská, B.; Bohdanecký, M.; Šebenda, J.; Tuzar, Z. Dilute Solutions of Nylon 12—II. Relationship between Intrinsic Viscosity and Molecular Weight. *Eur. Polym. J.* **1978**, *14*, 807–810. [[CrossRef](#)]
73. Nair, B. Final Report on the Safety Assessment of Benzyl Alcohol, Benzoic Acid, and Sodium Benzoate. *Int. J. Toxicol.* **2001**, *20*, 23–50. [[CrossRef](#)]
74. Gerike, P.; Gode, P. The Biodegradability and Inhibitory Threshold Concentration of Some Disinfectants. *Chemosphere* **1990**, *21*, 799–812. [[CrossRef](#)]
75. EFSA Panel on Food Additives and Flavourings (FAF); Younes, M.; Aquilina, G.; Castle, L.; Engel, K.-H.; Fowler, P.; Fürst, P.; Gürtler, R.; Gundert-Remy, U.; Husøy, T.; et al. Re-Evaluation of Benzyl Alcohol (E 1519) as Food Additive. *EFSA J.* **2019**, *17*, e05876. [[CrossRef](#)] [[PubMed](#)]
76. Wilson, L.; Martin, S. Benzyl Alcohol as an Alternative Local Anesthetic. *Ann. Emerg. Med.* **1999**, *33*, 495–499. [[CrossRef](#)] [[PubMed](#)]
77. Macht, D.I.; Nelson, D.E. On the Antiseptic Action of Benzyl Alcohol. *Proc. Soc. Exp. Biol. Med.* **1918**, *16*, 25–26. [[CrossRef](#)]
78. Meinking, T.L.; Villar, M.E.; Vicaria, M.; Eyerdam, D.H.; Paquet, D.; Mertz-Rivera, K.; Rivera, H.F.; Hiriart, J.; Reyna, S. The Clinical Trials Supporting Benzyl Alcohol Lotion 5% (Ulesfia™): A Safe and Effective Topical Treatment for Head Lice (*Pediculus Humanus Capitis*). *Pediatr. Dermatol.* **2010**, *27*, 19–24. [[CrossRef](#)]
79. Johnson, W.; Bergfeld, W.F.; Belsito, D.V.; Hill, R.A.; Klaassen, C.D.; Liebler, D.C.; Marks, J.G.; Shank, R.C.; Slaga, T.J.; Snyder, P.W.; et al. Safety Assessment of Benzyl Alcohol, Benzoic Acid and Its Salts, and Benzyl Benzoate. *Int. J. Toxicol.* **2017**, *36*, 5S–30S. [[CrossRef](#)] [[PubMed](#)]
80. Uragami, T.; Maekawa, K.; Sugihara, M. Studies on Syntheses and Permeabilities of Special Polymer Membranes. 21. Permeabilities of Alcohols and Hydrocarbons through Nylon 12 Membranes. *Angew. Makromol. Chem.* **1980**, *87*, 175–193. [[CrossRef](#)]
81. Uragami, T.; Maekawa, K.; Sugihara, M. Studies on Syntheses and Permeabilities of Special Polymer Membranes. XIV. Permeation Characteristics of Modified Nylon 12 Membranes. *Desalination* **1978**, *27*, 9–20. [[CrossRef](#)]
82. Funk, C.V.; Billovits, G.F.; Koreltz, M.S.; Dooley, J.; Chiou, N.-R. Inducing Surface Porosity in Aqueous-Quenched, Microporous Nylon 11 and Nylon 12 Films. *J. Appl. Polym. Sci.* **2017**, *134*, 44695. [[CrossRef](#)]
83. Tsai, C.-H.; Beltsios, K.; Cheng, L.-P. Formation of Bicontinuous, Hydrophobic Nylon 12 Membranes via Cold-Solvent-Induced Phase Separation for Membrane Distillation Application. *J. Appl. Polym. Sci.* **2019**, *136*, 47036. [[CrossRef](#)]
84. Yadykova, A.Y.; Ilyin, S.O. Rheological and Adhesive Properties of Nanocomposite Bitumen Binders Based on Hydrophilic or Hydrophobic Silica and Modified with Bio-Oil. *Constr. Build. Mater.* **2022**, *342*, 127946. [[CrossRef](#)]
85. Scott, R.L. The Thermodynamics of High Polymer Solutions. IV. Phase Equilibria in the Ternary System: Polymer—Liquid 1—Liquid 2. *J. Chem. Phys.* **1949**, *17*, 268–279. [[CrossRef](#)]
86. Krigbaum, W.R.; Carpenter, D.K. Phase Equilibria in Polymer—Liquid 1—Liquid 2 Systems. *J. Polym. Sci.* **1954**, *14*, 241–259. [[CrossRef](#)]
87. Minton, A.P. Simple Calculation of Phase Diagrams for Liquid—Liquid Phase Separation in Solutions of Two Macromolecular Solute Species. *J. Phys. Chem. B* **2020**, *124*, 2363–2370. [[CrossRef](#)] [[PubMed](#)]
88. Doi, M.; Edwards, S.F.; Edwards, S.F. *The Theory of Polymer Dynamics*; Clarendon Press: Oxford, UK, 1988; ISBN 978-0-19-852033-7.
89. Touris, A.; Turcios, A.; Mintz, E.; Pulugurtha, S.R.; Thor, P.; Jolly, M.; Jalgaonkar, U. Effect of Molecular Weight and Hydration on the Tensile Properties of Polyamide 12. *Results Mater.* **2020**, *8*, 100149. [[CrossRef](#)]
90. Hejmady, P.; van Breemen, L.C.A.; Hermida-Merino, D.; Anderson, P.D.; Cardinaels, R. Laser Sintering of PA12 Particles Studied by In-Situ Optical, Thermal and X-ray Characterization. *Addit. Manuf.* **2022**, *52*, 102624. [[CrossRef](#)]
91. Hansen, C.M. *Hansen Solubility Parameters: A User's Handbook*, 2nd ed.; CRC Press: Boca Raton, FL, USA, 2007; ISBN 978-0-429-12752-6.

92. Kallio, K.J.; Hedenqvist, M.S. Ageing Properties of Polyamide-12 Pipes Exposed to Fuels with and without Ethanol. *Polym. Degrad. Stab.* **2008**, *93*, 1846–1854. [[CrossRef](#)]
93. Beerbower, A.; Wu, P.L.; Martin, A. Expanded Solubility Parameter Approach I: Naphthalene and Benzoic Acid in Individual Solvents. *J. Pharm. Sci.* **1984**, *73*, 179–188. [[CrossRef](#)]
94. Macknight, W.J.; Karasz, F.E. Polymer Blends. *Compr. Polym. Sci. Suppl.* **1989**, *7*, 111–130. [[CrossRef](#)]
95. Chung, T.-S. The Limitations of Using Flory-Huggins Equation for the States of Solutions during Asymmetric Hollow-Fiber Formation. *J. Membr. Sci.* **1997**, *126*, 19–34. [[CrossRef](#)]
96. Ilyin, S.O.; Yadykova, A.Y.; Makarova, V.V.; Yashchenko, V.S.; Matveenکو, Y.V. Sulfonated Polyoxadiazole Synthesis and Processing into Ion-Conducting Films. *Polym. Int.* **2020**, *69*, 1243–1255. [[CrossRef](#)]
97. Wang, D.-M.; Venault, A.; Lai, J.-Y. Fundamentals of Nonsolvent-Induced Phase Separation. In *Hollow Fiber Membranes*; Elsevier: Amsterdam, The Netherlands, 2021; pp. 13–56. ISBN 978-0-12-821876-1. [[CrossRef](#)]
98. Matsuyama, H.; Karkhanечи, H.; Rajabzadeh, S. Polymeric Membrane Fabrication via Thermally Induced Phase Separation (TIPS) Method. In *Hollow Fiber Membranes*; Elsevier: Amsterdam, The Netherlands, 2021; pp. 57–83. ISBN 978-0-12-821876-1. [[CrossRef](#)]
99. Gorbacheva, S.N.; Yadykova, A.Y.; Ilyin, S.O. Rheological and Tribological Properties of Low-Temperature Greases Based on Cellulose Acetate Butyrate Gel. *Carbohydr. Polym.* **2021**, *272*, 118509. [[CrossRef](#)] [[PubMed](#)]
100. Shahzad, K.; Deckers, J.; Boury, S.; Neirinck, B.; Kruth, J.-P.; Vleugels, J. Preparation and Indirect Selective Laser Sintering of Alumina/PA Microspheres. *Ceram. Int.* **2012**, *38*, 1241–1247. [[CrossRef](#)]
101. Zhu, P.; Zhang, H.; Lu, H. Preparation of Polyetherimide Nanoparticles by a Droplet Evaporation-Assisted Thermally Induced Phase-Separation Method. *Polymers* **2021**, *13*, 1548. [[CrossRef](#)]
102. Gorbacheva, S.N.; Yadykova, A.Y.; Ilyin, S.O. A Novel Method for Producing Cellulose Nanoparticles and Their Possible Application as Thickeners for Biodegradable Low-Temperature Greases. *Cellulose* **2021**, *28*, 10203–10219. [[CrossRef](#)]
103. Parnian, P.; D'Amore, A. Fabrication of High-Performance CNT Reinforced Polymer Composite for Additive Manufacturing by Phase Inversion Technique. *Polymers* **2021**, *13*, 4007. [[CrossRef](#)]
104. Anokhina, T.S.; Ilyin, S.O.; Ignatenko, V.Y.; Bakhtin, D.S.; Kostyuk, A.V.; Antonov, S.V.; Volkov, A.V. Formation of Porous Films with Hydrophobic Surface from a Blend of Polymers. *Polym. Sci. Ser. A* **2019**, *61*, 619–626. [[CrossRef](#)]

Disclaimer/Publisher's Note: The statements, opinions and data contained in all publications are solely those of the individual author(s) and contributor(s) and not of MDPI and/or the editor(s). MDPI and/or the editor(s) disclaim responsibility for any injury to people or property resulting from any ideas, methods, instructions or products referred to in the content.